Macromolecules

ARTICLE

pubs.acs.org/Macromolecules

Surface-Induced Micelle Orientation in Nafion Films

Maria Bass,[†,‡] Amir Berman,[§] Amarjeet Singh,[⊥,∥] Oleg Konovalov,[⊥] and Viatcheslav Freger*[,†,‡,§]

[†]Zuckerberg Institute for Water Research, Ben-Gurion University of the Negev, Sde-Boqer Campus, Sde-Boqer 84990, Israel

[‡]Unit of Environmental Engineering and [§]Department of Biotechnology Engineering, Ben-Gurion University of the Negev, P.O. Box 635, Beer-Sheva 84105, Israel

[⊥]European Synchrotron Radiation Facility, ID10B, 6 Rue Jules Horowitz, BP-220, 38043 Grenoble CEDEX, France

ABSTRACT: Grazing incidence SAXS (GISAXS) was used to examine the surface structure of thin Nafion films spin-cast on hydrophobic silanized Si substrate and exposed to water and vapor. GISAXS spectra at low subcritical incidence angles, indicative of a few nanometers thick surface region, showed that in vapor Nafion micelles at the surface tend to align parallel to the surface, while under water they are preferentially oriented normal to the surface, in agreement with previously proposed structural picture and with AFM and contact angle results. However, spectra at near-critical incidence angles representing the bulk of the films indicate the micelles preferentially align normal to the surface, regardless of the external phase. This observation is in contrast with previous studies that employed hydrophilic native Si substrates, in which the observed micelle orientation was parallel to the surface. The proposed explanation assumes that lateral interactions with octadecyl tails and/or heterogeneities at the silanized Si surface, could be responsible for perpendicular alignment in the present case. The heterogeneities could allow preferential interactions of the substrate with both microphases of Nafion, rather than with one microphase, as in the case of bare Si. The observed effect of substrates on micelle orientation suggests an attractive possibility of enhancing transport within Nafion films in a desired direction.

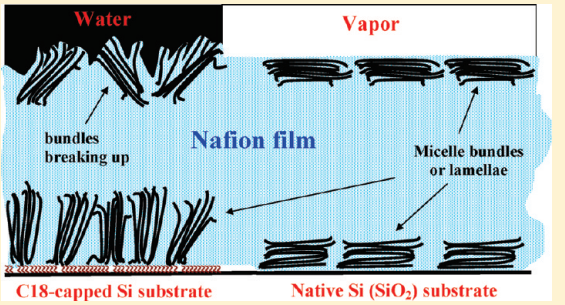

1. INTRODUCTION

Nafion is an ionomer widely used as an ion-selective barrier. It has attracted much attention due to its importance as a benchmark proton-conducting membrane material for fuel cells and other electrochemical applications.[1−6] The unique characteristics of Nafion originate from its chemical structure comprising a perfluorinated backbone and sulfonic groups (Figure 1). These highly incompatible constituents separate to microphases and form micelles, which may be of either normal or inverted type, depending on the level of hydration. Both types of micelles were shown to have a 2D morphology, i.e., have one dimension much longer than the other two and assume either the shape of rod-like aggregates in a continuous aqueous phase or bundled water nanochannels in a continuous polymer matrix. [Referring to the presence or absence of a bore these may be called "spaghetti" and "macaroni bundles", respectively, using a pasta terminology.] The former are characteristic of Nafion solutions, while the latter are often found in a solid Nafion.[7−12]

Hydration of Nafion exhibit many puzzling features, many of which seem to originate from the extremely long relaxation times of the perfluorinated Nafion matrix, which behaves as a quasi-elastic solid at time scales of weeks and months. As a result, Nafion usually rapidly reaches a quasi-equilibrium hydration state, in which the matrix is still able to support the elastic stress caused by expanding aqueous microphase that "inflates" the matrix.[13,14] Only after a much longer equilibration, the viscoelastic matrix slowly yields to the inflation stress and rearranges approaching a true equilibrium (relaxed) state. In water or saturated vapor such true equilibrium state is apparently the dilute solution of rod-like micelles ("spaghetti"). However, at ambient temperature such micelles form and disentangle from the matrix extremely slowly and in most applications Nafion retains a solid quasi-equilibrium state for very long times.

The true equilibrium in water may however be approached much more closely in a few nanometers-thick outermost surface region, which is subject to weaker topological constraints and additional surface tension forces. Such arguments were used recently to show that micelles in the surface region may be entrapped in entirely different metastable states depending on whether the polymer is exposed to saturated vapor or liquid water.[14,15] This may explain the often observed differences in hydration in these two modes of equilibration (the so-called Schroeder paradox[4,5,16−27]). The proposed picture and the structural ("macaroni-spaghetti") transition[15] that occurs when the environment changes from vapor to water are schematically shown in Figure 2.

Grazing incidence SAXS (GISAXS) is a powerful technique highly suitable for studying nanostructure and morphology of thin polymer films[28−30] and interfaces.[31,32] Using this method, a direct evidence of micelle arrangement at the Nafion surface

Received: October 15, 2010
Revised: January 31, 2011
Published: March 30, 2011

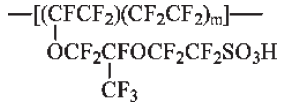

Figure 1. Chemical structure of Nafion, $m = 6.5$ for equivalent weight 1100 g/mol.[1]

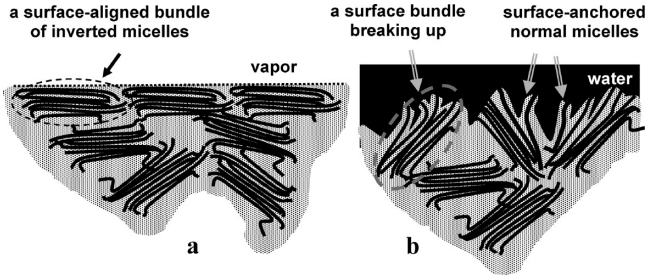

Figure 2. Structure of (a) Nafion-vapor and (b) Nafion-water interface schematically showing the breakup of surface-aligned bundles to separate micelles upon transfer from liquid to water ("macaroni-spaghetti" transition).[14,15]

was recently obtained and was corroborated by complementary measurements of contact angle and surface topography by AFM in vapor and under water.[15] The results were consistent with the assumption that Nafion micelles at the surface facing a vapor phase tend to align parallel to the surface and form a thin hydrophobic "crust". However, this evidence was incomplete in the sense that GISAXS was performed only in vapor thereby no direct comparison with the surface structure under water was made. Such experiments are presented in this report. To allow measurements under water the setup, X-ray beam energy, and the Si substrate had to be modified with respect to the previous GISAXS measurements in vapor. Therefore, apart from confirming the proposed surface structure, an important part of the present study was to properly address possible effects that could result from these changes, especially, in the substrate.

2. EXPERIMENTAL SECTION

Sample Preparation. Nafion films about 100 nm thick were prepared by spin-casting on Si wafers (15 × 15 mm^2) made hydrophobic via silanization with octadecyl trichlorosilane (OTS). For silanization, the wafers were successively sonicated and dried in 0.5 M HCl, toluene, acetone, and ethanol for 15 min in each solution. Dry wafers were then placed in 1 mM solution of OTS in molecular sieve-dried toluene at 4 °C for at least 24 h and thereafter cleaned by sonication in neat toluene. The clean hydrophobisized wafers showed a contact angle 105 ± 1° (OTC-20 contact angle analyzer, DataPhysics) using a 5 μL sessile drop. The spin-cast samples were prepared on a EC 101 spin-coater (Headway Research) at a rotation speed 3500 rpm using a 5% commercial solution of Nafion of equivalent weight 1100 g/mol in a mixture of water and low alcohols and ethers (Aldrich-Sigma) and then annealed at 160 °C for 3−5 days.

GISAXS Experiments. Scattering experiments were carried out at ESRF (Grenoble, France) at the ID10B beamline. The incident beam energy was 22 keV (wavelength $\lambda = 0.56$ Å); the energy was higher than in the previous study[33] in order to minimize scatter by the bulk water during measurements at the Nafion−water interface. In experiments under water samples were mounted horizontally at the bottom of a liquid cell filled with deionized water and fitted with X-ray transparent fluoropolymer windows. In experiments in vapor the sample was mounted horizontally inside a homemade temperature and humidity controlled chamber with Kapton windows.[15] A vertical position sensitive detector (PSD) was used and rotated horizontally around the sample to scan the 2δ angle in the horizontal $X-Y$ direction (parallel to the sample surface). GISAXS spectra were recorded at several incidence angles α_i, below, near, and above the critical angle α_c. The latter was estimated using the formula[31]

$$\alpha_c = Q_c\lambda/4\pi \quad (1)$$

where Q_c is the critical wavenumber estimated as explained in section 3; the value of α_c was also confirmed using the position of the Yoneda peak (see Results and Discussion). For each α_i the scan included about 90 δ values in the range $0.12° \le 2\delta \le 5°$ with a 60 s exposure for each δ value; no filter was used. In order to minimize the effect of radiation damage the sample was translated laterally by about 1 mm and realigned for each incident angle. Background scattering for the liquid cell (tests under water) and humidity chamber (tests in vapor) was measured using a horizontal beam ($\alpha_i = 0$) passing above the sample. Measurements under water were performed at room temperature and those in vapor at 30 °C. To prevent water condensation on the sample surface the relative humidity in the chamber was maintained at 97% using a saturated K_2SO_4 solution with excess K_2SO_4 filling a small water reservoir inside the chamber that was kept at the same temperature as the sample and the whole chamber (30 °C). Prior to measurements the samples were equilibrated inside the chamber for about 1.5 h. This time was presumably sufficient for the thin Nafion film to reach the quasi-equilibrium hydration (see the Introduction).

AFM Experiments. The surface of spin-cast Nafion films was scanned using a MultiMode Nanoscope III (DI-Veeco) in tapping mode in air and under water at ambient temperature. The samples were first scanned in air using RTESP Si probes (Veecoprobes) with nominal tip radius 8 nm that were used at their fundamental resonance frequency which typically varied from 200 to 400 kHz. Thereafter the same samples were covered with water and allowed to equilibrate overnight and scanned under water using SNL tips of nominal radius 2−3 nm and nominal resonance frequency 20 kHz. Different tips were used to achieve maximal resolution subject to difference in tip-surface interaction in respective medium. In either case the tip radius was much smaller than observed features.

3. RESULTS AND DISCUSSION

3.1. The Value of Critical Angle and Depth of Penetration in Water and Vapor. Since the amplitude of the evanescent wave at subcritical incidence angles $\alpha_i < \alpha_c$ exponentially decays within the film with the distance from the surface, most of the GISAXS signal comes from the surface region of a thickness commensurate with the penetration depth[31,32,34]

$$d_p \approx \frac{2}{Q_c\sqrt{1-(\alpha_i/\alpha_c)^2}} = \frac{2d_{\min}}{\sqrt{1-(\alpha_i/\alpha_c)^2}} \quad (2)$$

where $Q_c = 4\pi\alpha_c/\lambda$ is the critical wavenumber and $d_{min} = 1/Q_c$ is the minimal penetration depth. Dosch et al.[32] pointed out that in general a scattering length Λ that depends on the exit angle α_f as well should be used in place of d_p, especially for $\alpha_f < \alpha_c$; for instance, Λ does not becomes very large and stays commensurate with d_{min} even for $\alpha_i > \alpha_c$, if $\alpha_f < \alpha_c$. However, most features of interest in this study are found in the Q_z range above the Yoneda peak, for which $\alpha_f > \alpha_c$ and $\Lambda \approx d_p$. Equation 2 also neglects X-ray absorption, however, the equation provides a good approximation of d_p as long as α_i is not too close to α_c and $\alpha_f < \alpha_c$. In

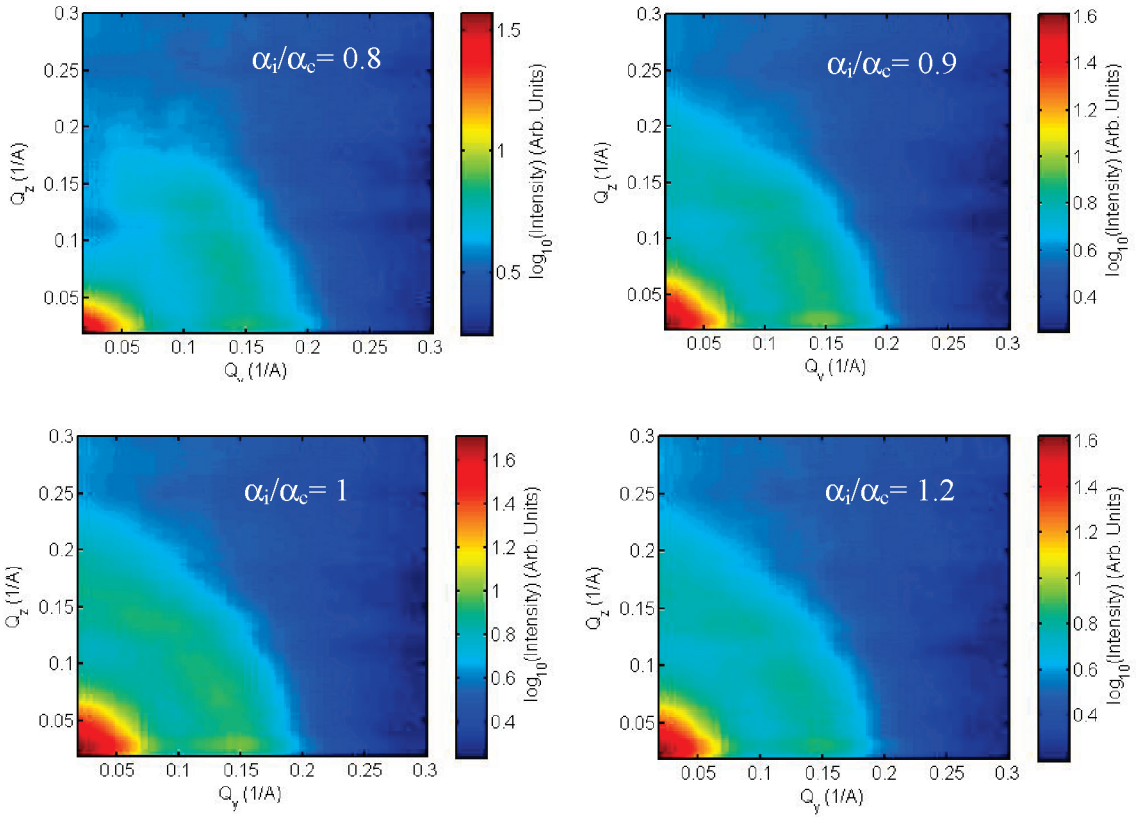

Figure 3. 2D GISAXS maps for the surface of a Nafion film (spin-cast on OTS-treated Si) under water for different incident angles. Beam energy 22 keV. The values of α_i/α_c are based on critical angle 0.05°.

particular, it shows that d_p stays within about twice $2d_{min}$ for $\alpha_i \leq 0.9\alpha_c$ and within only 25% above $2d_{min}$ for $\alpha_i \leq 0.6\alpha_c$.

When the incident beam comes from a medium with a substantial electron density such as water, Q_c is given by

$$Q_c = (Q_{c1}^2 - Q_{c2}^2)^{1/2} \quad (3)$$

where are Q_{c1} and Q_{c2} are the critical wave numbers at the interface with vacuum of the Nafion film (1) and the medium (2), respectively. The critical wave numbers are related to the electron density of the respective phase ρ_e as follows[31]

$$Q_{c1,2} = 4\sqrt{\pi r_0 \rho_{e1,2}} \quad (4)$$

where $r_0 = 2.8 \times 10^{-15}$ m is the classic radius of electron. The electron density of Nafion, calculated from known chemical composition and density, yields $Q_c \approx Q_{c1} \approx 0.029-0.03$ Å^{-1} for dry Nafion in vapor ($Q_{c2} \approx 0$), i.e., $d_{min} \approx 33-35$ Å. On the basis of the value $Q_{c2} \approx 0.0217$ Å^{-1} for water for the dry polymer under water, one expects $Q_c \approx 0.019$ Å^{-1} and $d_{min} \approx 53$ Å. These Q_c values are verified below.

Figures 3 and 4 show 2D GISAXS intensity maps obtained for Nafion films on OTS-treated Si wafers for different incidence angles in water and in vapor, respectively. In order to address the change in diffuse background scattering that increased with incidence angle and facilitate comparison between spectra the logarithmic color scale of intensity in Figure 3 and in Figure 4 was rigidly shifted for all spectra to match the background intensity at large Q. The feature of interest is the diffuse ring at $Q \approx 0.15-0.2$ Å^{-1}, the so-called ionomer peak, whose position and asymmetry are indicative of the micelle spacing and orientation. According to eqs 1 to 4, the critical angles for the beam energy 22 keV is about 0.07° in vapor and 0.05° in water. These values were calculated for a dry polymer and they could be smaller due to hydration. It has been shown previously that in vapor the external surface is depleted of ionic species thereby the estimate based on dry polymer well represents the conditions at the surface.[15] However, under water the film and, in particular, its surface was expected to be significantly hydrated. If the film in water contained as much water as Nafion 117 membrane (22 water molecules per sulfonic group[16]), α_c is expected to drop to about 0.04° and it was unclear whether the lowest angle used under water (0.04°) was indeed subcritical.

However, the critical angle could be estimated directly from GISAXS maps on the basis of the fact that the intensity is enhanced when either α_i or α_f or both are close to α_c.[31,34] First, the overall intensity in the 2D spectra under water was clearly the largest at $\alpha_i = 0.05°$ (Figure 3), which strongly suggests that α_c was close to this value. Second, the position of the Yoneda peak seen as a horizontal streak in the lower part of the spectra and corresponding to $Q_z = (Q_c + Q_i)/2$, where $Q_i = 4\pi\alpha_i/\lambda$, was used as well to make an estimate of α_c. This estimate was also in favor of α_c being close to 0.05° rather than to the lower value expected for hydrated Nafion. This result is only taken here as an evidence that spectra for $\alpha_i < 0.05°$ in Figure 3 correspond to subcritical conditions. Nevertheless, it might also indicate that hydration and density of Nafion in the thin films on the solid hydrophobic substrate used in this study might be lower than for thick bulk films.

3.2. Arrangement of Micelles at Interface with Water and Vapor. The ionomer ring in the spectra shown in Figure 3 gradually becomes isotropic with the increase of incidence angle.

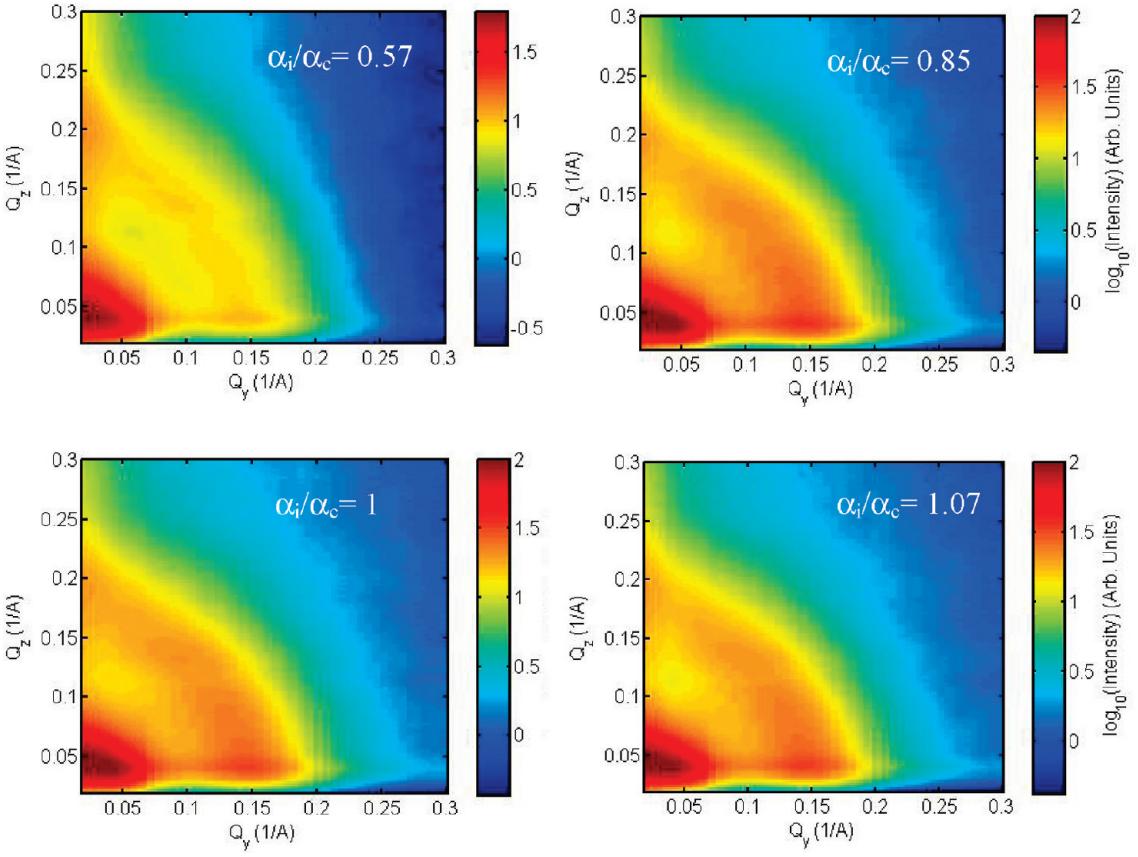

Figure 4. GISAXS map for the surface of a Nafion film (spin-cast on OTS-treated Si) in vapor for different incident angles. Beam energy 22 keV. The values of α_i/α_c are based on critical angle 0.07°.

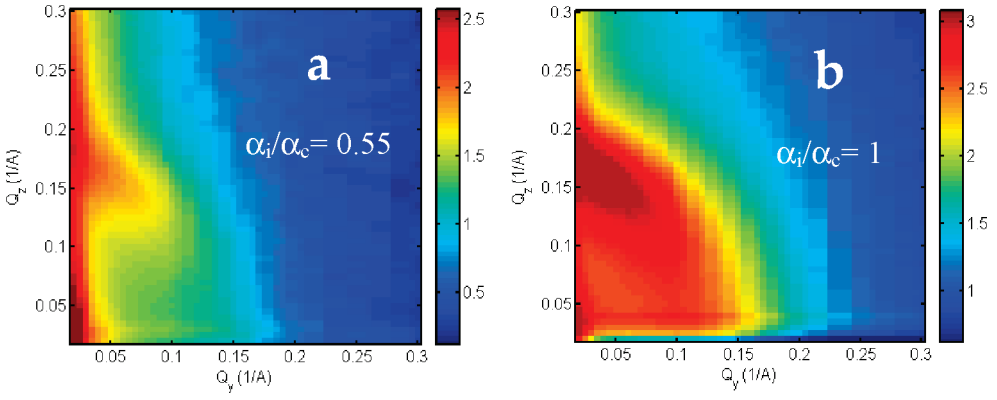

Figure 5. GISAXS maps for the surface of a Nafion film spin-cast on untreated native Si in vapor for an undercritical (a) and critical (b) incident angles. Beam energy 8 keV. The values of α_i/α_c are based on critical angle 0.20°.[15]

However, at $\alpha_i/\alpha_c < 1$ the vertical (Z) component of the ionomer ring is noticeably weakened, indicating preferred upright orientation of micelles at the surface in water. Equation 2 shows that the scattering at subcritical angles predominantly comes from a surface region a few nanometers thick. This thickness is of the order of the intermicelle spacing, which means the micelles adjacent to the polymer−water interface are preferentially oriented *normal* to the surface. This agrees well with the proposed structural picture of the Nafion surface in water, whereby the polymer directly facing water phase is expected to break up to individual micelles. This breakup is incomplete and the micelles do not fully disentangle and remain anchored at one end to the film (Figure 2b). They then only have freedom to extend to the water phase, while their lateral spacing remains restricted and similar to the micelle spacing in the solid bulk. Such arrangement, somewhat resembling a polymer brush,[35] should lead to predominant orientation of micelles normal to the surface. This should result in weakening of the ionomer peak in Z direction for subcritical incidence angles without as much effect in the XY direction, as indeed observed.

This pattern is in marked contrast with the case of Nafion surface exposed to vapor, in which case the micelles arrange

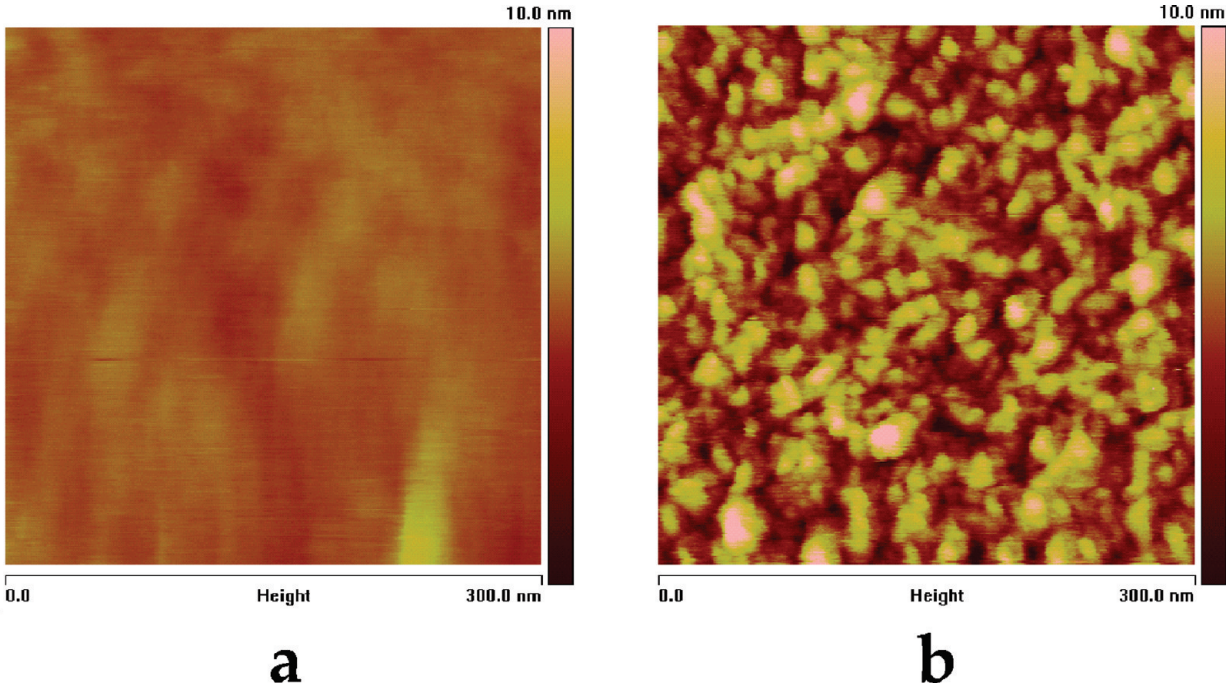

Figure 6. Topographic AFM images of the surface of a Nafion film (a) in vapor and (b) under water. The film was spin-cast on an OTS-treated Si wafer. The images were flattened using a 2nd order line-to-line routine. The rms roughess after flattening is 0.35 and 1.85 nm, respectively.

parallel to the surface, which results in the ionomer peak enhanced in Z and weakened in XY direction at subcritical α_i. This was shown previously using vapor-exposed Nafion films spin-cast on *hydrophilic* bare Si using a beam of lower energy (8 keV, $\alpha_c \approx 0.20°$). Although Q_c is independent of the beam energy, a different *hydrophobic* substrate used in this study could make a difference. It could also be possible that the lower beam energy and lower incidence angles (22 keV, $\alpha_c \approx 0.07°$) could make the experiments more prone to uncertainties related to surface roughness. Therefore, in order to verify previous conclusions and consistently compare samples exposed to water and vapor, GISAXS spectra were also recorded in vapor for Nafion films on the *hydrophobic* substrate using the beam energy identical to experiments under water. The results are shown in Figure 4. It is seen that the scattering pattern at the lowest measured angle $\alpha_i = 0.04° \approx 0.6\alpha_c$ well compares with previous data (see Figure 5a). The ionomer peak in Figure 5a is similarly enhanced in *Z* direction relative to *XY*, which indicates that the micelles in the outmost region tend to align parallel to the surface and make the surface as flat as possible.

The drastic change that the surface undergoes when transferred from vapor to under water could also be directly observed using AFM. Compared to the previous study, sharper tips were used to obtain an improved resolution. The topographic images shown in Figure 6 visualize the marked difference between the relatively flat Nafion surface in ambient air (Figure 6a) and a much rougher surface under water (Figure 6b). The surface under water developed small asperities, which increased the rms roughness about 5-fold compared to vapor. The asperities were apparently formed in the process of breakup to small individual aggregates ("macaroni−spaghetti" transition) (Figure 2). Although individual asperities under water are still several times larger than individual micelles, even such an incomplete breakup may be already sufficient to bring about the preferential orientation observed in GISAXS spectra.

3.2. Orientation of Micelles within the Film. When the incidence angle approaches and exceeds α_c the GISAXS spectrum becomes representative of the bulk of the film rather than the surface region. In the previous study[15] it was observed that on hydrophilic bare Si substrate (covered with a native SiO_2 layer) the micelle in a thin Nafion exposed to vapor were predominantly oriented parallel to the substrate both in the bulk and at the surface (Figure 5b). This was in full agreement with the recent neutron reflectivity results by Dura et al. who reported a strong *parallel* orientation of Nafion adjacent to solid hydrophilic substrates.[36] Moreover, they could conclude from their data that in the vicinity of a bare Si substrate hydrated Nafion adopts a lamellar morphology, whereby dense lamellae are separated by thin water-rich layers *parallel* to the substrate. The aqueous layer between the first lamella and hydrophilic substrate on bare Si could cause a rapid detachment of Nafion film under water, which was indeed observed. Apparently, for that reason experiments under water were only successful using a hydrophobic OTS-treated substrate, in which case Nafion films could sustain prolonged immersion in water.

However, inspection of GISAXS maps for films on OTS-treated substrates, both in water (Figure 3) and in vapor (Figure 4), shows that the use of a different substrate in this study brought about an unexpected change in the bulk morphology. In particular, the ionomer peak is consistently weakened in Z direction for near- and overcritical incidence angles. This indicates that micelles in the bulk are predominantly oriented *perpendicular* to the substrate. This is especially remarkable in vapor, in which case orientation changes from parallel at the surface to perpendicular in the bulk. Apparently, the micelle orientation within the bulk of the films beyond the thin outmost surface region was mostly controlled by the interface with the substrate rather than by the external surface.

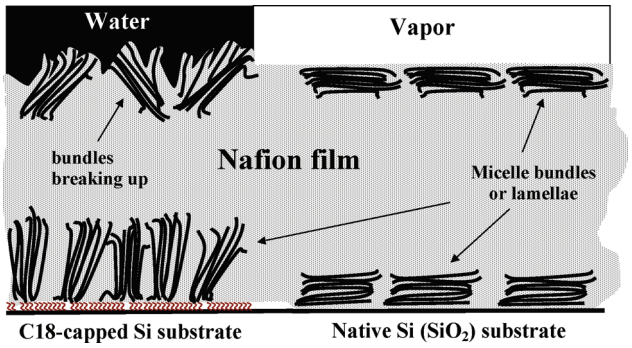

Figure 7. Schematic representation of micelle arrangement within Nafion in contact with various media.

It could be assumed that this hydrophobic OTS-treated substrate was in a direct contact with the hydrophobic matrix of Nafion which water could not disrupt. Since the C18 tails within the OTS layer are known to self-align nearly normal to the substrate surface,[37] it is likely that their orientation could promote alignment of the adjacent Nafion backbone chains and, ultimately, micelles. Such alignment could be facilitated by lateral interactions with small defects in the OTS layer. Small nanometer-scale islands of bare hydrophilic substrate might also form a pattern that promotes normal orientation of Nafion micelles. Even though the OTS-treated surface was overall hydrophobic (contact angle 105°), hydrophilic nanoislands or similar imperfections are typically present within OTS monolayers self-assembled on a native SiO_2.[38,39] In this case, normal orientation could be stabilized by the heterogeneity of the OTS-treated surface leading to preferential interaction of the two microphases of Nafion with imperfections. For instance, the aqueous "cores" of the micelles (water nanochannels[12]) could preferentially interact with hydrophilic islands, while hydrophobic surface fraction surrounding the islands would preferentially attract with the hydrophobic Nafion "shells". Obviously, a homogeneous bare Si surface would be unable to induce such heterogeneous interaction patterns and would be more likely to preferentially interact with only one microphase leading to parallel alignment of micelles, as was indeed observed.[15,36]

It is seen that both substrate and external phase appear to affect morphology and orientation of the Nafion micelles. Figure 7 schematically illustrates and summarizes the suggested surface structures. Depending on the properties of the adjacent phase, the observed morphology and arrangement may vary from parallel to the interface (lamellae on native SiO_2 of Si substrate and "macaroni" bundles at polymer−vapor surface) to perpendicularly oriented "macaroni" on a C18-capped Si substrate and surface-anchored loose "spaghetti" at the interface with water. The possibility to control morphology and orientation of nanochannels within Nafion films using an appropriate substrate could be highly attractive for enhancing its transport properties and ionic conductivity in desired direction. This effect could be likened to enhanced transport of gases, water and various solutes through membranes built of arrays of aligned carbon nanotubes.[40,41]

CONCLUSIONS

GISAXS experiments with thin Nafion films on hydrophobic Si substrate allowed comparison of surface structure of Nafion in vapor and under water. This comparison at subcritical incidence angles showed that in vapor environment Nafion micelle at the surface preferentially align parallel to the surface, while under water they are oriented normal to the surface, in agreement with previously proposed structural picture and with AFM and contact angle results.

Unexpectedly, GISAXS spectra at near-critical incidence angles indicate that in the bulk of the films the micelles tend to align normal to the surface, regardless of the external phase. This observation is in contrast with micelle alignment parallel to the surface that was previously observed on hydrophilic native Si substrates. It is assumed here that the difference could originate from interaction with the C18 tails of OTS aligned normal to the substrate surface and from surface heterogeneities and defects present in the hydrophobic OTS layer on native hydrophilic Si surface. Such heterogeneities could allow preferential interactions of the substrate with both microphases of Nafion, rather than with one microphase, as in the case of bare Si.

The results suggest an attractive possibility of enhancing the performance of thin Nafion membranes through preferential alignment of micelles using patterned substrates. Since ion and water mobility should be the largest along the micelles, surface-treated nanopatterned substrates might be potentially useful for enhancing ionic conductivity and water transport within Nafion membrane in the desired direction.

AUTHOR INFORMATION

Corresponding Author

*E-mail: vfreger@bgu.ac.il.

Present Addresses

[||]Department of Physics, Banasthali University, Banasthali 304022, Rajastan, India.

REFERENCES

(1) Mauritz, K. A.; Moore, R. B. *Chem. Rev.* **2004**, *104* (10), 4535–4585.
(2) Costamagna, P.; Srinivasan, S. *J. Power Sources* **2001**, *102* (1−2), 253–269.
(3) Perry, M. L.; Fuller, T. F. *J. Electrochem. Soc.* **2002**, *149* (7), S59–S67.
(4) Broka, K.; Ekdunge, P. *J. Appl. Electrochem.* **1997**, *27* (2), 117–123.
(5) Zawodzinski, T. A.; Derouin, C.; Radzinski, S.; Sherman, R. J.; Smith, V. T.; Springer, T. E.; Gottesfeld, S. *J. Electrochem. Soc.* **1993**, *140* (4), 1041–1047.
(6) Diat, O.; Gebel, G. *Nat. Mater.* **2008**, *7*, 13–14.
(7) Aldebert, P.; Dreyfus, B.; Gebel, G.; Nakamura, N.; Pineri, M.; Volino, F. *Journal De Physique* **1988**, *49* (12), 2101–2109.
(8) Gebel, G. *Polymer* **2000**, *41* (15), 5829–5838.
(9) Rubatat, L.; Rollet, A. L.; Gebel, G.; Diat, O. *Macromolecules* **2002**, *35* (10), 4050–4055.
(10) Rubatat, L.; Gebel, G.; Diat, O. *Macromolecules* **2004**, *37* (20), 7772–7783.
(11) Gebel, G.; Diat, O. *Fuel Cells* **2005**, *5* (2), 261–276.
(12) Schmidt-Rohr, K.; Chen, Q. *Nat. Mater.* **2008**, *7* (1), 75–83.
(13) Freger, V. *Polymer* **2002**, *43* (1), 71–76.
(14) Freger, V. *J. Phys. Chem. B* **2009**, *113* (1), 24–36.
(15) Bass, M.; Berman, A.; Singh, A.; Konovalov, O.; Freger, V. *J. Phys. Chem. B* **2010**, *114* (11), 3784–3790.
(16) Bass, M.; Freger, V. *Polymer* **2008**, *49* (2), 497–506.
(17) Choi, P.; Jalani, N. H.; Datta, R. *J. Electrochem. Soc.* **2005**, *152* (3), E84–E89.
(18) Choi, P. H.; Datta, R. *J. Electrochem. Soc.* **2003**, *150* (12), E601–E607.
(19) Cornet, N.; Gebel, G.; de Geyer, A. *J. Phys. IV* **1998**, *8* (P5), 63–68.
(20) Elfring, G. J.; Struchtrup, H. *J. Membr. Sci.* **2007**, *297* (1−2), 190–198.

(21) Freger, V.; Korin, E.; Wisniak, J.; Korngold, E. *J. Membr. Sci.* **2000**, *164* (1−2), 251–256.
(22) Hinatsu, J. T.; Mizuhata, M.; Takenaka, H. *J. Electrochem. Soc.* **1994**, *141* (6), 1493–1498.
(23) Jeck, S.; Scharfera, P.; Kinda, M. *J. Membr. Sci.* **2009**, *337*, 291–296.
(24) Onishi, L. M.; Prausnitz, J. M.; Newman, J. *J. Phys. Chem. B* **2007**, *111* (34), 10166–10173.
(25) Schroeder, P. V. *Z. Phys. Chem.* **1903**, *45*, 75.
(26) Vallieres, C.; Winkelmann, D.; Roizard, D.; Favre, E.; Scharfer, P.; Kind, M. *J. Membr. Sci.* **2006**, *278* (1−2), 357–364.
(27) Weber, A. Z.; Newman, J. *J. Electrochem. Soc.* **2003**, *150* (7), A1008–A1015.
(28) Lazzari, R. *J. Appl. Crystallogr.* **2002**, *35* (4), 406–421.
(29) Lee, B.; Park, I.; Yoon, J.; Park, S.; Kim, J.; Kim, K.-W.; Chang, T.; Ree, M. *Macromolecules* **2005**, *38* (10), 4311–4323.
(30) Müller-Buschbaum, P. *Anal. Bioanal. Chem.* **2003**, *376* (1), 3–10.
(31) Als-Nielsen, J.; McMorrow, D., *Elements of Modern X-ray Physics*; John Wiley & Sons: New York, 2001.
(32) Dosch, H.; Batterman, B. W.; Wack, D. C. *Phys. Rev. Lett.* **1986**, *56* (11), 1144.
(33) Bass, M.; Berman, A.; Singh, A.; Konovalov, O.; Freger, V. *J. Phys. Chem. B* **2010**, *114* (11), 3784–3790.
(34) Vineyard, G. H. *Phys. Rev. B: Condens. Matter* **1982**, *26* (8), 4146.
(35) Milner, S. T. *Science* **1991**, *251* (4996), 905–914.
(36) Dura, J. A.; Murthi, V. S.; Hartman, M.; Satija, S. K.; Majkrzak, C. F. *Macromolecules* **2009**, *42* (13), 4769–4774.
(37) Sagiv, J. *J. Am. Chem. Soc.* **1980**, *102* (1), 92–98.
(38) Balgar, T.; Bautista, R.; Hartmann, N.; Hasselbrink, E. *Surf. Sci.* **2003**, *532*, 963–969.
(39) Bautista, R.; Hartmann, N.; Hasselbrink, E. *Langmuir* **2003**, *19* (17), 6590–6593.
(40) Hinds, B. J.; Chopra, N.; Rantell, T.; Andrews, R.; Gavalas, V.; Bachas, L. G. *Science* **2004**, *303* (5654), 62–65.
(41) Holt, J. K.; Park, H. G.; Wang, Y. M.; Stadermann, M.; Artyukhin, A. B.; Grigoropoulos, C. P.; Noy, A.; Bakajin, O. *Science* **2006**, *312* (5776), 1034–1037.